Can riparian vegetation shade mitigate the expected rise in stream temperatures due to climate change during heat waves in a pre-alpine river?

Heidelinde Trimmel[1], Philipp Weihs[1], David Leidinger[1], Herbert Formayer[1], Gerda Kalny[2]

[1]Institute of Meteorology, University of Natural Resources and Life Science (BOKU), Vienna, 1190, Vienna, Austria
[2]Institute of Soil Bioengineering and Landscape Construction (IBLB), University of Natural Resources and Life Science (BOKU), Vienna, 1190, Austria

Correspondence to: Heidelinde Trimmel (heidelinde.trimmel@boku.ac.at)

Abstract. The influence of expected changes in heat wave intensity during the 21st century on the temperatures of an pre-alpine river are simulated and the mitigating effects of riparian vegetation shade on the radiant and turbulent energy fluxes were analysed. Stream water temperature increases of less than 1.5°C were modelled within the first half of the century. For the period 2071–2100 a more significant increase of around 3 °C in maximum, mean and minimum stream temperature was predicted for a 20 year return period heat event. Additional riparian vegetation was not able to fully mitigate the expected temperature rise caused by climate change, but could reduce maximum, mean and minimum stream temperatures by 1 to 2 °C. Removal of existing vegetation amplified stream temperature increases. Maximum stream temperatures could increase by more than 4 °C even in yearly heat events.

Keywords: stream temperature, modelling, riparian vegetation, shade, climate change

1 Introduction

Stream temperature is an important factor influencing the physical, chemical and biological properties of rivers and thus the habitat use of aquatic organism (Davies-Colley and Quinn 1998; Heino et al. 2009; Magnuson et al. 1979). Studies suggest that freshwater biodiversity is highly vulnerable to climate change with extinction rates exceeding those of terrestrial taxa (Heino et al. 2009). Stream temperature and assemblages of fish and benthic invertebrates along the river course are highly correlated. The duration and magnitude of especially the maximum summer stream temperatures are limiting factors for many species occurrence (Matulla et al. 2007, Melcher et al. 2014, Melcher et al. 2016).

Continuous warming of water temperatures induce changes in fish assemblages and slow altitudinal shifts of species, if the habitat is suitable and no migration barriers exist. River continuum disruption reduces the fish zone extent significantly. Extreme events where lethal thresholds of stream temperature are exceeded can cause exchange of zoonoses or even extinction of species (Melcher et al. 2013, Pletterbauer et al. 2015). The largest uncertainties in forecasts of total suitable habitat are climate uncertainty (Wenger et al. 2013). Above that riparian ecosystems play a superior role in determining the vulnerability of natural and human systems to climate change in the 21st century (Capon et al. 2013).

Air temperatures have been rising and are expected to continue to rise globally within the next century (IPCC 2013). In eastern Austria in the period since 1880 mean air temperature has risen by 2 °C, which is more than double the 0.85 °C rise recorded globally (Auer et al. 2014). A further temperature increase within the 21st century is very likely (APCC 2014). A mean air temperature increase of 1.4 °C within the first half of the century is expected in Austria (Ahrens et al. 2014). Temperature development thereafter is strongly dependent on future greenhouse gas emissions. If emission scenario A1B is assumed, mean air temperature increases of 3.5 °C by the end of the 21st century are expected in Austria (APCC 2014, Gobiet et al. 2014). Other scenarios predict higher (A2) or lower (B1) increases (Gobiet et al. 2014).

Temperatures extremes have changed markedly and extreme high temperature events i.e. heat waves are very likely to increase in the 21st century (APCC 2014).

According to IPCC (2013) precipitation has the tendency to decrease in subtropical regions but increase in the middle latitudes on average. Austria lies between these two zones of opposing trends. Northern Europe shows an increasing trend, while the Mediterranean has a decreasing trend (IPCC 2013, Böhm 2006). In southeastern Austria a precipitation decrease of about 10–15 % has been recorded over the last 150 years (APCC 2014, Böhm 2012). The decrease has been observed in summer (Apr – Sep) and winter (Oct – Mar) (Böhm et al. 2009, 2012). A continuation of this trend might aggravate the danger of summer drought. In eastern Austria low flow discharge rates of rivers is likely to decrease by 10 to 15% for 2021–2050 compared to 1976–2007 during all seasons (Nachtnebel et al. 2014).

Heavy and extreme precipitation shows no clear increasing signal on average, but it is likely to increase from October to March (APCC 2014). Various studies indicate that from observations no long term increase of wind speed or storm activity can be detected in Europe (e.g. Matulla et al. 2008). For the alpine region also no clear signs of increasing wind speed or extremes are projected for the future (Beniston et al. 2007). An increase of sunshine hours in the Alps has been modelled, but no similar signal has been found for the low lands (Ahrens et al. 2014).

Stream temperature is controlled by advection of heat, dispersion and the net energy fluxes acting on the surface and river bed. While net short wave radiation is the dominant energy input causing diurnal and seasonal water temperature variability, long wave radiation flux as well as the turbulent fluxes evaporation and convection, which are controlled by air humidity, air temperature, wind and net radiation, play an important role (Caissie et al. 2007; Garner et al 2014; Hannah et al. 2008; Johnson 2004; Trimmel et al. 2016). Water temperature is sensitive to air temperature changes (Hannah et al. 2008) so that even if global radiation, air humidity and wind have no clear climate change signal, the change in air temperature alone will affect stream temperatures significantly (Nachtnebel et al. 2014; Settele et al. 2014; van Vliet et al. 2016). Apart from this soil temperature is expected to increase due to climate change and will influence stream temperatures via substrate heat conduction and groundwater flux (Kurylyk et al. 2015). For example, in Austria near surface groundwater body temperature is expected to rise by 0.5 to 1 °C on average by 2050 (BMLFUW 2011).

Since 1980 230 stations of the Austrian hydrographic central office of different elevation, distance from source and catchment area recorded an increase of stream temperature. The data were elevation corrected using External Drift Top-Kringing (Skøien et al. 2006) and a mean trend calculated using the Mann-Kendall-Test (Burn and Hag Elnur, 2002) by BMLFUW (2011). A mean trend of

1.5 °C during summer (Jun - Aug) and 0.7 °C during winter (Dec - Feb) was calculated (APCC 2014, BMLFUW 2011).

Melcher et al. (2013) analysed 60 stations and found a similar trend of 1 °C within the last 35 years regarding mean August temperatures, which was independent of the river type. The annual mean temperature of the river Danube has been rising (Webb and Nobilis 1995) and is likely to continue to rise to reach a value between 11.1 and 12.2 °C by 2050 compared to around 9 °C at the beginning of the 20th century at the border to Slovakia (Nachtnebel et al. 2014). Close to Vienna the increase will be up 12.7 °C (Dokulil 2013). Due to the size of the river Danube amplitudes and extremes cannot be compared to smaller rivers like Pinka, but trends in mean water temperature values are comparable (BMLFUW, 2011).

Precipitation changes which affect discharge volume in general and the indirect effects of climate change on stream temperature like the percentage contributions of surface, subsurface, groundwater and/or snow melt still have to be analysed in more detail (Johnson and Wilby 2015). For the study region during summer heat waves neither groundwater nor snow melt contributions change are expected (APCC). Apart from rising air temperatures and discharge changes, anthropogenic influences like discharge from waste water treatment plants and cooling water can influence stream temperatures in a negative way and are therefore presently illegal in Austria (WRG 1959). Other consequences of climate change are changes in sediment loads in river systems due to changes in mobilization, transport and deposition of sediment, which is expected to be very likely (APCC 2014). Sediment changes might alter the bed conduction flow as well as flow velocity, which can influence the magnitude and variability of stream temperature. Artificial changes which deteriorate the situation are presently illegal in Austria as well (WRG 1959).

Discharge reductions on the other hand have already been observed. From 1982 to 1990 the mean discharge of the river at the lower boundary of the study region decreased by 5.7 % (Mader et al. 1996) and has been further decreasing (APCC 2014). During the period 2008-2012 the mean discharge lay 20% below the values of 1982 (BMLFUW 2014). Van Vliet (2011) predicted a stream temperature rise of 0.3 °C and 0.8 °C on average for discharge reductions of 20 % and 40 % respectively.

This article focused only on the increase in air temperature caused by climate change.

One of the most influential factors regulating stream temperature is riparian vegetation (Caissie 2006, Groom et al. 2011; Johnson 2004; Moore et al. 2005; Rutherford et al. 1997). Streamside vegetation buffer width (Clark et al. 1999), vegetation density and average tree height all have a strong influence on stream temperature (Sridhar et al. 2004). Vegetation affects the sky view of the river and thereby short and long wave radiation flux, evaporation and convection heat flux, who are highly correlated to the openness of the sky, which can be evaluated using the view to sky value (VTS). The VTS can be influenced by factors other than vegetation such as topographic obstructions and bank shade (Boyd and Kasper 2003, Trimmel et al. 2016).

The main energy input during heat wave conditions is short wave radiation and the most significant output of stream energy occurs via evaporation. The reduction of short wave radiation can contribute significantly to reduce the heating of rivers during warmer summers (Sinokrot and Stefan 1993; Parker and Krenkel 1969; Rutherford et al. 1997; Trimmel et al. 2016). Vegetation can reduce the incoming global radiation by up to 95% (Holzapfel et al. 2013). Evaporation is dependent on the difference between water and air temperature, relative humidity, wind speed – which is affected by the roughness of the environment – and net radiation. An obstructed sky view reduces net incoming radiation, but it also reduces wind speed, air humidity and air temperature gradients and consequently evaporation. Long wave outgoing radiation and convective heat flux are dependent on the level of openness to the sky as well. During sunny conditions sky obstructed sites have reduced energy fluxes compared to open sites. (Benyahya et al. 2012; Garner et al. 2014; Hannah et al. 2008; Trimmel et al. 2016, Webb et al. 2008). Transpiration of riparian vegetation only indirectly affects stream temperature. It increases air humidity and reduces air temperature close to the river, so air humidity and air temperature gradients are reduced. Benyahya et al. (2012) and Chen et al. (1993), recorded a difference in air humidity between open and forested stations of 5 % and 11 % and a difference of air temperature in 0.5 % and 0.61 °C respectively.

Apart from its influence on average stream temperature vegetation produces highly spatial variable shade, which results in areas of different sun exposure and energy fluxes. These heterogeneity provides ecological niches which are important for different development stages of river fauna(Clark et al. 1999). In particular, the maximum water temperatures during heat waves are reduced significantly by vegetation shade (Garner et al. 2014)

Though the influence of vegetation on water temperature is evident, its ability to mitigate climate change is not yet sufficiently understood.

There are different approaches to predicting stream temperature. Water temperature can be predicted using statistical functions (stochastic models) and its correlation (regression models) to known variables (e.g. air temperature, water temperature of the previous days or streamflow). Use of air temperature as a surrogate for future water temperature can lead to errors when linear (Erickson and Stefan 2000; Webb and Nobilis 1997) or non-linear (Mohseni et al. 1998) regression models are applied (Arismendi et al. 2014). Stochastic models used to determine the long term annual component of temperatures and their short term residuals separately yielded good results (Caissie et al. 2001). Including a discharge term in the regression model improves the model's performance during heat wave and drought (low flow) conditions, when water temperatures are most sensitive to air temperature (van Vliet et al. 2011).

Energy balance models resolving all energy fluxes affecting a river system are the best suited to predict stream temperature (Caissie et al. 2007) but demand the most input data. These models are able to simulate energy flux changes caused by increased or decreased river shade.

The conclusion may be drawn that many studies have already addressed the influence of riparian vegetation on stream water temperature using field measurements. Other studies coped with different methods to predict stream temperature and few tried to answer the question on how climate change might increase stream water temperature. Mainly air temperature was used as a surrogate for stream temperature and energy flux variations at different river sections were not considered. One result or trend may however not be transferred from one river to other. Statements of the riparian vegetation's potential to mitigate influence of climate change are only reliably valid for a given type of stream and for a given climate zone. The novel aspect of the present study is to investigate the influence of climate change and of riparian vegetation on the same river and attempt to make a realistic forecast of the riparian vegetation's potential to mitigate climate change in a specific river.

The aim of the present article is therefore (1) to estimate the magnitude of stream temperature rise during extreme heat events caused by the expected rise in air temperature until the end of this century compared to the last observed period and (2) to investigate the ability of riparian vegetation to mitigate the expected water temperature rise.

2 Methods

Preliminary work has been done and published by Holzapfel and Rauch (2015), Holzapfel et al. (2015) and during a different article by Trimmel et al. (2016). Vegetation cover and river morphology was recorded continuously along the river, stream temperatures were recorded at 12 sites as well as main tributaries of the eastern Austrian river Pinka (Holzapfel and Rauch 2015, Holzapfel et al. 2015). This data was used to set up and validate the 1D energy balance and hydraulic model Heat Source (Boyd and Kasper 2003) for the river Pinka (Trimmel et al. 2016).

Further Heat Source was used to analyse the mean influence of different meteorological, hydrological and shading parameters during heat wave conditions along a 22.5 km long uniform reach (Trimmel at al. 2016).

In the present article stream temperature was simulated with the 1D energy balance and hydraulic model Heat Source (Boyd and Kasper 2003) for 51 km along a section including upstream forested regions and tributaries for each 500m along the river, which amounts to a total of 103 sites. First the longitudinal changes of energy fluxes were analysed during the maximum heat wave, which took place in eastern Austria during summer 2013. Future heat wave episodes, which are likely to occur during the climate periods 2016-2045, 2036-1065 and 2071-2100 in the study region, were selected. Regional climate scenarios, which have been produced within the ENSEMBLE project (Hewitt et al. 2004) were further processed and the meteorological data extracted. The future upstream model water temperature was simulated according the methodology of Caissie et al. (2001). Heat Source was used to simulate the stream temperature of the river Pinka for 12 future episodes and three vegetation scenarios.

2.1 Study region

The river Pinka originates at 1480 meters above sea level (m.a.s.l.) in the eastern Austrian Alps and discharges about 100 km downstream at 200 m. a. s. l. into the river Raab. The catchment size of Pinka is 664 km². According to Muhar et al (2004), who categorized all Austrian rivers with catchment areas > 500 km² corresponding to their annual discharge, Pinka falls in the smallest of the 5 categories with 0 – 5 $m^3 s^{-1}$ mean annual discharge. The study region covers a 51 km stretch of the river Pinka from distance from source (DFS) 11 (559 m.a.s.l) near its most upstream gauge in Pinggau 1 (to DFS 62 (240 m.a.s.l.) close the gauge at Burg) (Fig. 1). In the first 10km the river has a slope of 0.017 m m^{-1} whereas in the remaining section the slope is only 0.004 m m^{-1}. The river bankfull width varied from 4 to 10 m. The maximum depth of the different river sections varied between 0.1 and 0.5 m and was 0.17 m on average.

In this region air temperature rose by 2 °C, since 1880. Precipitation was reduced in the HISTALP region corresponding to our study region by 10-15%, which is the largest reduction in precipitation in Austria (Auer et al. 2007, Böhm et al. 2009, Böhm et al. 2012).

2.2 Modelling energy balance and stream temperature along the river

Using the deterministic energy balance and hydraulic model Heat Source version 9 (Boyd and Kasper, 2003; Garner 2007) and topographic, vegetation, river morphology, hydrological and meteorological data sets, the energy fluxes along the river, hydraulics and stream temperature were simulated along the Pinka. Existing data sets and parameters obtained from Austrian authorities and the literature were completed with field surveys and measurements. Short and long wave energy flux, latent and sensible heat flux as well as conduction are taken into account:

$$\Phi_{\text{Total}} = \Phi_{\text{Latent}} + \Phi_{\text{Sensible}} + \Phi_{\text{Longwave}} + \Phi_{\text{Solar}} + \Phi_{\text{Conduction}} \quad (1)$$

where Φ_{Total} is the energy balance, Φ_{Latent} the latent heat flux, Φ_{Sensubke} the sensible flux, Φ_{Longwave} the long wave radiation balance all referring to the stream surface, Φ_{Solar} is the short wave energy which is absorbed by the water column and $\Phi_{\text{Conduction}}$ the conduction flux to the stream bed. Latent heat flux was calculated using the Penman method, which included the radiation balance.

The effect of the energy balance of the water column on stream temperature was calculated by Heat Source taking into account flow velocity and river morphology. The stream temperature increase ΔT caused by Φ_{Total} was calculated using:

$$\Delta T = \frac{\Phi_{\text{Total}} * \text{dt}}{\left(\frac{A}{W_w}\right) * c_{H2O} * m} \quad (2)$$

where A is the cross sectional area or the river, W_w is the wetted width, the c_{H20} is the specific heat capacity of water (4182 J kg^{-1} C^{-1}), m the mass of 1 m^3 water which is 998.2 kg.

The model had been adapted and validated for usage at the Pinka during heat wave conditions by Trimmel et al. (2016). The sensitivity of Heat Source towards all meteorological and shading input parameters was tested and the influence of vegetation, bank and topographic shade analysed by Trimmel et al. (2016).

By fine tuning the morphological input (bottom width, roughness parameter Manning's n and sediment hyporheic thickness) and the wind parametrisation, the model's validity could be considerably improved for the simulations used in this article. Tuning increased the coefficients of determination R^2 for stations analysed in Trimmel at al. 2016 from 0.87–0.91 (daily minimum), 0.90–096 (daily mean) and 0.86–0.92 (daily maximum) to 0.96–0.98 (daily minimum), 0.96–0.99 (daily mean) and 0.94–0.98 (daily maximum). The measurements fitted the simulation very well (hourly RMSE was 0.88 °C averaged for all stream measurement stations) so we concluded that all assumption were good and the model fit to be used for predictions.

2.3 Preparation of input

2.3.1 Meteorological input

During the maximum heat wave event of 2013, field measurements were collected at the study site. Global radiation, air temperature, air humidity and wind speed was measured at a reference station located at DFS 39 km 47° 16' 11.055" N 16° 13' 47.892" E, 300 m.a.s.l. (Trimmel et al. 2016). To link the measured micro scale meteorological data to topo scale meteorological data a systematic intercomparison between the local meteorological stations of the Austrian Weather Service (ZAMG) and the 1x1 km gridded observational data set INCA (Haiden et al., 2011) was done. Since the local permanent meteorological stations of ZAMG were used to produce the gridded INCA data set, they are highly consistent. The comparison of the INCA data with the air temperature measured at our reference station close to the river showed a RMSE of 0.67°C and a R^2 of 0.99 for consecutive hourly measurements during summer half-year 2013 (1 Apr – 30 Sept). So the INCA data set was used as proxy to represent the local meteorological conditions within the catchment.

To obtain future meteorological conditions data from the regional climate models (RCM) Aladin (driven by the global climate model ARPEGE), Remo and RegCM3 (both ECHAM 5 driven) for the location of the reference station were extracted. The aim was to estimate possible maximum temperature values, therefore data from Aladin, the climate model with the most extreme dry and hot summers, were selected. The RCMs were bias corrected using the quantile mapping technique (Déqué 2007) based on the E-OBS data set (Haylock et al., 2008) and scaled. In a second step the data were spatially localized to a 1 km x 1 km grid for the area encompassing the area under investigation using the Austrian INCA data set (Haiden et al. 2011). In a third step the data were temporally disaggregated from a resolution of one day to one hour. Temperature was disaggregated based on the daily maximum and minimum temperatures using three piecewise continuous cosine curves (Koutsoyiannis 2003, Goler & Formayer 2012). The temperature data were elevation corrected with a lapse rate of 0.65 °C per 100 m.

Selection of extreme heat events

The period chosen as past reference period ("OBS") was an extreme heat wave that ran from 4 – 8 August 2013, which was the most intense heat wave of the year 2013. The mean air temperature of this episode was comparable to a 20 year return period 5 day event (see section 2.3) for the period 1981–2010.

Future episodes were selected by choosing future heat wave events in three periods (2016–2045: "2030", 2036–2065: "2050", 2071–2100: "2085") in the summer months (June–August) that were simulated for the emission scenario A1B by the climate model Aladin (Radu et al. 2008). The events were chosen by selecting periods when the 5 day mean air temperature exceeded different thresholds using the percentiles of the 5 day mean air temperature of the three periods, which corresponded to an event with a 1 year (1a), 5 year (5a) or 20 year (20a) return period as well as the heat wave that represented the maximum event of the period (Max). The selection criteria are shown in Table 1. The start was 14 days prior to the end of the episode to allow spin up of the Heat Source model, so that all episodes have equal length of 14 days.

2.3.2 Vegetation and morphology

The riparian vegetation cover and river morphology of this region was investigated by Kalny et al. (2015), Holzapfel et al (2015) and Holzapfel and Rauch (2015). Vegetation height and density was sampled in a 50 m buffer on both sides of the river. Vegetation overhang, morphology of the river bank and bed were all recorded along the whole river stretch (Kalny et al. 2015; Trimmel et al. 2016). The riparian vegetation situation was taken after the phenological phase of leaf development was finished and leaves were already fully developed (Ellenberg 2012).The vegetation composition ranges from commercial spruce forests (Picea abies) close to the source and near natural deciduous riparian vegetation sections with willows (*Salix sp.*), poplars (*Populus sp.*), maples (*Acer sp.*), ash (*Fraxinus excelsior*), alder (*Alnus glutinos*a) and wild cherry (*Prunus sp.*) to highly altered sections with only one-sided sparse tree plantations of e.g. maples (*Acer sp.*) or lime trees (*Tilia sp.*) lining the river course.

Vegetation scenarios

To estimate the influence of different shading elements the following scenarios were used: no vegetation cover (V0), maximum vegetation cover (V100) and actual vegetation cover (STQ).

STQ used the best available status quo input data for vegetation, bank and topographic shade as described in Kalny et al. (2015) and above.

For V0 all vegetation parameters (vegetation height, density and overhang) were set to 0 so that no vegetation shading occurred. V100 was defined as: 30 m height and 8 m overhang and 90 % vegetation density. This scenario ensured the maximum possible vegetation shade. The fact that the density was below 100 % still enabled some exchange with the atmosphere. River bank and topography were not changed in the vegetation scenarios.

2.3.3 Definition of sediment layer and conduction flux

Heat Source uses only one substrate temperature, which is representative for the whole sediment layer. The depth of the sediment layer is set to 1m, which is corresponding to the available geological information of the river Pinka. The substrate temperature used in the model is set equal to the stream temperature at the uppermost model point. For each consecutive model point the substrate temperature is calculated depending on the local thermal conductivity, thermal diffusivity, layer depth, hyporheic exchange, the river morphological profile and the received solar radiation at the river bed. The sediment of this region is very inhomogeneous and the spatial distribution of the groundwater level is unknown (Pahr 1984). For low flow conditions it was assumed that there was no deep groundwater influence. .

2.3.4 Definition of discharge

During the analysed period 4 – 8 August 2013 low flow conditions were prevailing. The river flow volume increased from 0.18 m^3s^{-1} close to the upstream model boundary at DFS 13 to 0.76 m^3s^{-1} at the downstream model boundary (DFS 62). The mean flow velocity was 0.46 ms^{-1} and it took the river water about 30 hours to traverse the studied length of the river.

The model was very sensitive to discharge rates. A change in discharge of 0.1 m^3s^{-1} lead to a 4 times increase in stream temperature (0.4 °C) (Trimmel et al. 2016). Because the aim was to estimate the influence of vegetation shade, clear sky periods were chosen where no or only minor precipitation events occurred so discharge was fixed at mean low flow conditions (MLF). MLF is defined as the average discharge of all discharges below the 5% percentile discharge. The mean low flow conditions (MLF) of the gauging station Pinggau DFS 13 1981–2010 (MLF = 0.143 m^3s^{-1}), which is maintained by the Hydrographischer Dienst Österreich were used in the model. At the other end of the study region at DFS 62 the corresponding flow volume was 0.795 m^3s^{-1}.

2.3.5 Upstream boundary stream temperature

Stream temperature and discharge were used as upstream boundary condition. For the 2013 episode these values rely on observations. To obtain equivalent data for future conditions first the maximum water temperature was modelled at DFS 11 km using the expected air temperature as input (Mohseni et al., 1998). The water temperature was split into two components: the long term seasonal component (or annual component) and the short term non seasonal component (or residuals series) (Caissie et al. 2001). The annual component was calculated according to Kothandaraman (1971) and the residuals were calculated with a stochastic second-order Markov model after Cluis (1972) and Salas et al. (1980). Observed hourly water temperatures (12 537 values) over the period 7 July 2012 to 9 September 2014 were used to fit the model. The coefficient of determination R^2 between observed and predicted water temperature for this period was 0.96, the RMSE was 0.68 °C. For the summer half-year 2013 (Apr – Sept), the R^2 was 0.89, the RMSE was 0.80 °C. To take into account the climatic trend caused by the warming of the land surface (Kurylyk et al. 2015) the difference between the moving average of a 30 year climate period and the reference period 1981–2010 was added to the annual component.

2.3.6 Input data of tributaries

The discharge and water temperature of the river Pinka at the upstream model boundary and the main 5 tributaries of the 2013 episode were measured. The remaining tributaries added less than 5 % discharge each. Their future water temperature values were synthesised using the daily fluctuations of the water temperature at the upstream model boundary. adding a fixed offset depending on the distance of the inflow to the upstream model boundary. Missing discharge information was supplemented using percentages from the discharge at gauge Burg, as they were estimated during 2013.

2.4 Uncertainties in predicted stream temperature

As we already mentioned before, the model uncertainties of the Heat Source model were already determined in a previous study by Trimmel et al. (2016). The results will be used in the analysis of the present paper. In the following we give a short summary of the main results: The model is most sensitive to changes in vegetation height (+/-5 m), density (+/-20 %) and overhang (+/-1 m), which caused changes in water temperature of +/–0.40 °C, +0.44 /–0.46 °C and +0.01 /–0.05 °C respectively (Trimmel et al. 2016). The influence of bank shade on mean water temperature, not considering riparian vegetation, was calculated to be 0.31 °C, while the mere influence of topographic shade was estimated to be 0.44 °C. Existing vegetation on the other hand was found to be responsible for 4 times as much influence on temperatures as bank or topographic shade (1.68 °C) (Trimmel et al. 2016).

Microclimatic differences caused by vegetation shading, wind reduction and transpiration had been recorded during 5 July to 14 August 2015. Air temperature differences between forested and open stream reaches amounted to 1.5 °C on average. Differences in relative humidity were 11.8 % on average, which is in accordance with Benyahya et al. (2012) and Chen et al. (1993) , who recorded a difference in air humidity between open and forested stations of 5 % and 11 % and a difference of air temperature in 0.5 % and 0.61 °C respectively. Vegetation shading as well as the wind reduction caused by vegetation is included in the model. The micro scale changes in air temperature and air humidity of different river sections caused by transpiration are not included in the simulation, but Heat Source is not sensitive to these differences. Simulations were performed to estimate the error caused by this simplification and only a maximum error in water temperature of 0.18 °C was calculated.

3 Results

3.1 Influence of energy fluxes and vegetation shade on stream temperature during the heat episode 2013

In order to interpret the influence of vegetation shade on future water temperature it is important to understand the influence of vegetation shade on the present conditions first. While in the previous study of Trimmel et al. (2016) only the propagation of uncertainties of input parameters on the mean stream temperature of a 22.5 km long reach during the heat episode of 2013 was analysed, here the longitudinal distribution of a more diverse section including the headwaters of the river Pinka was shown and discussed.

The most important influences of atmospheric energy fluxes and vegetation shade on stream temperatures are depicted in Fig. 2.

The mean view to sky (VTS) for the study region under current conditions (STQ) was 0.55. If all vegetation was removed (V0) there was still some remaining shade caused by topography and the river bank which reduced VTS to a value of 0.89. If maximum vegetation was assumed (V100), the value of VTS was strongly reduced, but still amounted to 0.16 on average because only 90% density was assumed. Peaks in VTS were found at broader river sections or sections oriented East-West (Fig. 2a).

The most important energy inputs on the river surface during the study period and region were short wave radiation flux with an average of 101.6 W m^{-2} (Fig. 2a), sensible heat flux with an average of 39.9 W m^{-2} (Fig. 2e) and long wave radiation with an average of 17.2 W m^{-2} (Fig. 2c). Conduction only amounted to 1.3 W m^{-2} on average. The relative percentage of short wave radiation balance, long wave radiation balance and sensible heat flux were 64 %, 11 % and 25 % of the inputs respectively that heated the water column.

The main energy output was latent heat flux (Fig. 2f).

During the V0 and V100 scenario the direction of the energy fluxes remained the same. During the V0 scenario the relative percentage of short wave radiation balance increased (73 %), while long wave radiation balance (7 %) and conduction heat flux (18 %) decreased. During the V100 scenario the trend was opposite. Short wave radiation balance decreased (47 %) and long wave radiation balance (21 %) and sensible heat flux (32 %) increased (Fig. 2a-f).

Looking at the longitudinal distribution of energy fluxes along the river it can be seen that sensible heat flux and long wave radiation flux as well as conduction showed their highest values close to the source during all vegetation scenarios. This lead to a rapid increase in the water temperature of the cool spring water, which is clearly seen in both measured and simulated data (Fig. 2h).

All energy fluxes were dependent on the degree of openness to the sky, and showed the same pattern along the river (Fig. 2a - g). Short wave radiation and latent heat flux in particular were strongly influenced by the value of the VTS and showed distinct cutbacks of up to 70% where shading occurred (Fig. 2b, 2d).

The energy balance was positive on average along the whole river reach (Fig. 2g). The V0 scenario showed the highest, V100 scenario the lowest values with a mean value of 55, 40 and 22 W m^{-2} for the V0, STQ and V100 scenario respectively (Fig. 2g). The greatest differences between the different vegetation scenarios were found close to the source, where during the V0 scenario up to 200 W m^{-2} net energy were available to heat the water column (Fig. 2g), while during the V100 scenario it was only 91 W m^{-2}. The positive energy balance can explain the gradual warming of the stream temperature along the river (Garner et al. 2014) which can be seen in Fig. 2h. The continuous downstream warming is reversed on DFS 16, 22, 26.5, 32, 43.5 and 53.5 in the range of 0.5 °C for about 1 km (Fig. 2h) caused by the mixing with tributaries.

3.2 Future climate and advective input

The selection criteria mean air temperature increased depending on the return period of the event (Table 1, 2). Apart from the 1a and 5a events of 2030 and the 1a event of 2050 all events were warmer than the 2013 heat wave. Air humidity during the selected events decreased slightly until the end of the century, but had a value below average during the 2013 event (Table 2). The wind speeds of 2013 also exceeded the wind speeds of all future events (Table 2). In the 20 year return period event of 2050 wind speeds were higher (1.1 m s^{-1}) than in 2030 (0.9 m s^{-1}) and 2085 (0.8 m s^{-1}) (Table 2). The average global radiation received during each event per day was different for each event as well. For the 20 year return event 2030 (28 MJ m^{-2} d^{-1}) ie. global radiation was higher than 2050 (23.1 MJ m^{-2} d^{-1}) and 2085 (23.1 MJ m^{-2} d^{-1}). During the 20 year return event of 2085 on the other hand global radiation was higher than the Max event (20.9 MJ m^{-2} d^{-1}) of this climate period (Table 2).

For the mean water temperature at the model boundary an increase of +4.1 °C for a 20 year return event of 2085 in respect to 2013 was simulated (Table 2). For the Max event of 2085, which had 2.2 MJ m^{-2} d^{-1} lower global radiation input a slightly lower temperature increase (+4.0 °C) was simulated (Table 3).

The extraction of the future climate data were based on the location of the INCA grid. INCA data for the heat event in 2013 could be compared with data measured directly at the river. The INCA data assume a greater distance to the river surface and show higher mean and maximum air temperatures, but also lower air humidity and higher wind speed. This difference in meteorological input data resulted in a 0.1 °C higher water temperature (Table 3). Maximum water temperature was affected also, showing a reduction of 0.3 °C. Minimum water temperature was 0.6 °C warmer when INCA data input were used.

To be able to directly compare the 2013 event with the future scenarios, henceforth the simulation using the INCA data of 2013 is referred to as “20a OBS”.

3.3 Future stream temperatures

At DFS 39

To analyse future changes first the location of the reference station, which is positioned in the centre of the study region at DFS 39 km, was used. As a temporal reference the focus was placed on the 20 year return period events of the 2071–2100 climate period as it represents the maximum expected temperature rise.

The mean water temperature (Fig. 3, Table 3) of the river Pinka, MLF conditions and STQ at DFS 39 during the 20a heat wave event of the periods 2016–2045, 2036–2065 and 2071–2100 were predicted with 22.4 °C, 22.6 °C and 25.5 °C respectively. The corresponding predicted maximum water temperatures were 25.0 °C, 24.8 °C and 27.3 °C. These predictions represented a significant increase over the mean temperatures of the 20a event of the OBS period of 22.5 °C (maximum temperature: 24.4 °C) by the end of the century.

For mean temperatures a minor increase in water temperature was predicted for the first half of the century even for extreme heat events with a 20 year return period (Table 4). However, by the end of the century (2071–2100) a remarkable increase of +3 °C was modelled. Also maximum water temperatures showed increases. For the period 2016–2045, maximum temperatures increased more than mean temperatures with a change over baseline conditions of +0.6 °C. By 2071–2100 the increase in maximum temperatures was predicted to be 2.9 °C compared to the OBS period, which was similar to the predicted increase in mean and minimum water temperatures (Table 4).

Supposed the existing vegetation were removed (V0), the mean water temperature reached 26.7 °C during 20 year return period heat events at the end of the century, which was 4.2 °C above the level of the STQ scenario of the OBS period. Maximum temperatures could even reach 28.9 °C, which is 4.5 °C more than in STQ scenario of the OBS period (Fig. 3, Table 3, 4).

Supposed maximum riverine vegetation was implemented (V100) the expected mean water temperature was predicted to reach only 23.9 °C, which is 1.4 °C above the level of the STQ scenario during 2013 (Fig. 3,Table 3,4). The maximum temperature reached in this scenario is 25.5 °C which is only 1.1 °C above the maximum event of the OBS period (Fig. 3, Table 3, 4).

Vegetation was not able to compensate fully the temperature increase expected by the end of the century. For the climate period 2036–2065 though, riverine vegetation had the potential to more than compensate for climate change during extreme events and could even cause a reduced warming of –1.2 °C on average and –1.4 °C concerning maximum temperatures (Table 4).

Longitudinal distribution

The stream temperatures increased from the upstream model boundary at DFS 11 to DFS 62 during the 2013 heat wave event for the STQ scenario including all available information about the present state of the river was about 7° C (Fig. 2). Looking at the longitudinal distribution of water temperature along the river it can be seen that increases in mean stream temperature caused by increases of future air temperature affected all parts of the river (Fig. 4a-c).

The maximum values showed a similar distribution as the mean values on a higher level. The average difference between mean and maximum values of the STQ scenario was 3.92 °C, 3.35 °C and 3.91 °C, the maximum difference between maximum values was 5.51 °C, 4.89 °C and 5.51 °C and the standard deviation of this difference was 0.71, 0.66 and 0.71 for 2030, 2050 and 2085 respectively (Fig. 4a-c).

V0 scenarios were always warmer than STQ scenarios, V100 scenarios were always cooler than the STQ scenarios. The mean difference along the river between V0 and STQ was 1.25 °C, 1.26 °C and 1.13 °C, the maximum difference was 1.81 °C, 1.85 °C and 1.66 °C, the standard deviation was 0.35, 0.36 and 0.32 for 2030, 2050 and 2085 respectively. The mean difference between STQ and V100 was 1.42 °C, 1.52 °C, and 1.26 °C, the maximum difference was 1.92 °C, 2.05 °C and 1.72 °C, the standard deviation of this difference was 0.46, 0.49 and 0.41 for 2030, 2050 and 2085 respectively (Fig. 4A-c).

Water temperature was especially sensitive to the removal of vegetation within the first 10 km (DFS 11 - 21) where there were dense forests which prevented the cool headwaters from warming (Fig. 4d). At DFS 11 - 21 temperatures increased by 1.4 °C when removal of vegetation is assumed (V0-STQ). Additional tree cover (V100) caused a reduction of -0.9 °C compared to the STQ scenario (Fig. 4d).

This can be explained by the slower flow velocities (last 30 km - DFS 32-62: 0.003 m m^{-1}, 0.4 m s^{-1}) in comparison to the steeper upstream sections (first 10 km - DFS 11-21: 0.017 m m^{-1}, 0.6 m s^{-1}), which gave short wave radiation in unshaded sections more time to heat the water column.

For the Pinka the benefit of additional tree cover maximizing riparian shade became more distinct in the downstream sections (DFS 25-55) where the additional tree cover caused a change of 1.75°C while removal only caused a change of around 1.25°C (Fig. 4d).

4 Discussion

4.1 Energy fluxes during heat waves

In the present article evaporative heat flux was responsible for 100 % of the heat loss on average. Short wave radiation balance, long wave radiation balance and sensible heat flux were 64 %, 11 % and 25 % of the inputs respectively that heated the water column.

During summer periods of high air temperature difference between air and water temperature increases, which can trigger intensified evaporative flux that cools the river, but also can cause sensible heat flux to heat the water column (Benyahya et al. 2012). Benyahya et al. 2012 measured during 7-23 June 2008 evaporative heat flux to account for 100 % of energy outputs while short wave radiation balance, long wave radiation balance and sensible heat flux were 73 %, 25 % and 3 % of the inputs respectively that heated the water column.

4.2 Magnitude of stream temperature rise

In the present article for a heat wave with 20 year return period in the climate period 2071–2100 with +3.8 °C increase in air temperature in respect to the observed period and MLF discharge, increases in maximum, mean and minimum stream temperatures of close to +3 °C in respect to the observed period were simulated for DFS 39. During the Max event increases of maximum, mean and minimum values where 3.4 °C, 3.5 °C and 4 °C respectively. When looking at the whole river mean changes of 3.3 °C for the maximum and 3.9 °C mean temperatures were calculated. Melcher et al (2014) also found that average and maximum temperatures show similar warming trends. An increase of 3.9°C from the OBS period to 2085 corresponds to an increase of 0.43 °C/decade. An increase of 3°C to an increase of 0.33 °C/decade.

The relatively low values of water temperature predicted for the 20a 2050 heat wave might be explained by higher wind speeds and lower air humidity causing higher evaporation rates and lower solar radiation energy input compared to 2013. This was most evident in maximum water temperatures. For the V0 scenario low water temperatures were also predicted, which would support the idea of increased evaporation. The maximum vegetation scenario shows comparably warm stream temperatures in respect to 2013.

From 1980 to 2011 230 stations of the Austrian hydrographic central office of different elevation, distance from source and catchment area recorded an increase of stream temperature (BMLFUW 2011).

For Austrian rivers summer stream temperature increased by 1.5 ° C between 1980 and 2011 according to this study (BMLFUW 2011) (0.48 °C / decade).

Melcher et al (2013) found a trend of 1°C within the last 35 years regarding mean August temperatures independent of the river type (0.29 °C / decade).

Dokulil (2013) extrapolated the quadratic regression of the period 1900-2006 of the river Danube near Vienna and predicted an increase of up to 3.2 °C by 2050 in respect to 1900 (0.21 °C / decade). Using linear regression the increase was only 2.3 (0.15 °C / decade), but using the linear trend beginning from 1970 the increase was 3.4° C (0.23 °C / decade). Due to the size of the river Danube daily amplitudes and extremes are not comparable to the Pinka, but trends in mean water temperature values are comparable though.

The values predicted in this article were clearly above the model uncertainty and lie in the upper region of the values published by other studies (BMLFUW 2001, Dokulil 2013, Melcher et al. 2013, 2014) .

Considering a likely discharge decrease (Nachnebel et al. 2014) slightly higher temperature rise might be expected. Van Vliet et al. (2011) analysed 157 river temperature stations globally for the 1980–1999 period and predicted increases of annual mean river temperature of 1.3 °C, 2.6 °C and 3.8 °C under air temperature increases of 2 °C, 4 °C and 5 °C respectively. Discharge decreases of 20 % and 40 % increased the water temperature rise by 0.3 °C and 0.8 °C on average (Van Vliet et al. 2011).

4.3 Ability of riparian vegetation to mitigate the expected stream temperature rise

Vegetation scenarios were simulated. Compared to the STQ scenario, additional riparian vegetation (V100) could reduce maximum stream temperatures during all episodes on average by 2.2 °C, mean by 1.6 °C and minimum by 0.9 °C during extreme heat waves (calculated from Table 4). Removal of existing vegetation (V0) amplified stream temperature increases, and could cause an average increase of maximum, mean and minimum stream temperatures by 1.8 °C, 1.3 °C and 1.0 °C respectively in comparison with the actual vegetation scenario (STQ) (calculated from Table 4).

Removal of vegetation (V0) magnified the stream temperature during 20 year return period events by the end of the century by up to 4.2 °C (mean) and 4.5 °C (daily maximum). Additional riparian vegetation (V100) on the other hand mitigated part of the rise in maximum temperatures, so there was only a 1.1 °C increase. The increase of mean temperatures was reduced to about 1.4 °C, so riparian vegetation management alone was not enough to compensate for the predicted warming caused by climate change.

The reduction rates predicted in the present article lie within the range of observed changes of pre- and post harvest situations found in literature (Cole and Newton 2013; Moore et al. 2005).

The water temperature difference between full and no vegetation showed no clear trend for future conditions. This can be explained considering that global radiation - the main parameter, that is affected by riparian vegetation (Leach and Moore 2010, Li et al 2012) - is the main parameter that contributes to heating of the water column (Benyahya et al 2012, Hannah et al. 2008, Maheu et al. 2014) and is not expected to be affected by climate change (APCC 2014).

Therefore the ability of the vegetation to alter the stream's microclimate and water temperature is likely to remain the same.

4.4 Limitations

Attention has to be given to the fact that vegetation mainly causes reduction of maximum stream temperatures by reducing the solar radiation input at the river surface by shading. This effect is strong during times of clear skies and high solar irradiation. During cloudy skies and during night time this effect is less pronounced while outgoing long wave radiation is still impeded by the sky obstruction caused by vegetation. This in turn could lead to higher mean and minimum temperatures, which can be also seen in the simulated events of low global radiation.

Although vegetation can have important effects on stream temperature, there will be river sections which will not be affected by the addition (or removal) of vegetation due to upstream or lateral, surface or subsurface advection of heat or topographic shade (Johnson and Wilby 2015). Ground water influence was unknown and no ground water influence was assumed in the model. Although the model performed good (RMSE 0.88) there might be some ground water influence between DFS 45 and 55 where the measurements lie below the simulation results.

Not tackled were other aspects related to future development and climate change, such as potential but not predictable anthropogenic heat sources or sinks as discharge of tempered waste water, possible changes in stream velocity and shading as sediment changes caused by impoundments, regulation and canalization as well as feasible discharge changes such as withdrawal of water for irrigation. The climate input was using only one possible emission scenario simulated by one regional climate model.

5 Conclusions

In this study the influence of expected changes in heat wave intensity during the 21st century on stream temperature in the rithron to upper potamal river section of the eastern Austrian river Pinka were simulated and the mitigating effect of riparian vegetation shade on the radiant and turbulent energy fluxes was analysed.

By the end of the century (2071–2100) in the study region an air temperature increase of 3.8 °C to 5.6 °C was predicted during annual or less frequent extreme heat waves in comparison to the observed period of 1981–2010.

Stream water temperature increases of less than 1.5 °C were modelled for the first half of the century. For the period 2071–2100 a more significant increase of 3 °C in maximum, mean and minimum stream temperatures was predicted for a 20 year return period heat event..

Vegetation could reduce stream temperature during heat waves, where high solar radiation is usual. Additional riparian vegetation was not able to fully mitigate the expected temperature rise caused by climate change, but could reduce maximum stream temperatures by 2.2 °C, mean by 1.6 °C on average during extreme heat waves. Removal of existing vegetation amplified stream temperature increases, and could cause an increase of maximum and mean stream temperatures by 1.8°C and 1.3 °C respectively in comparison with the actual vegetation scenario on average.

Removal of vegetation showed to aggravate the situation. Assuming vegetation removal maximum stream temperatures could exceed a 4 °C increase compared to the observed period in annual heat events at the end of the century.

There might be counterproductive effects of full vegetation cover on stream water temperatures during periods of reduced solar radiation, which can increase stream temperature, but generally riparian vegetation can produce important thermal gradients in streams which are vital for many species (Clark et al. 1999).

This study shows that it is very likely that during extreme events an increase of 2 °C, which is the magnitude of the temperature differentiation of the local fish zones (Melcher et al. 2013, Pletterbauer et al. 2015), will be exceeded during this century. At a stream temperature of 20 °C, cold water adapted species reach their lethal phase (Melcher et al. 2014, Schaufler 2015). During a simulated annual heat wave event in the period 2016–2035 this threshold was never exceeded in the most upstream region (DFS13), which is presently populated by the cold adapted species brown trout (Guldenschuh 2015). At the end of the century during a heat wave event of a 20 year return period the threshold was likely to be exceeded for 72 of 120 h. At the lower boundary of the trout zone (DFS 20) during heat waves 20°C already were exceeded for 70 of the 120 h at the beginning of the century, but could be reduced by riparian vegetation shade during annual heat events to only last 9 h in total. The mitigation possibilities of vegetation were limited though, and could not fully compensate for the whole predicted temperatures rise. At the end of the century in heat waves of a 5 year or less frequent return period, even if maximum vegetation was assumed, 20 °C was exceeded during the whole heat wave event.

Team list (alphabetical order): Herbert Formayer, Clement Gangneux, Gerda Kalny, David Leidinger, Andreas Melcher, Imran Nadeem, Hans Peter Rauch, Heidelinde Trimmel, Philipp Weihs, David Whittaker

Code availability: The last official version of the used software TTools and Heat Source are available online at: http://www.deq.state.or.us/WQ/TMDLs/tools.htm
The changes included into Heat Source within this study will be implemented in the next version, which will be available at the same location.

Data availability: The simulation input and result data sets for the present and future heat wave episodes used in this article are part of the research project BioClic and will be published together with the other vegetation, morphological and biological data sets produced in the project on the freshwater biodiversity data portal (http://data.freshwaterbiodiversity.eu/) and receive a doi.

Authors contributions: Weihs P. helped to better understand the energy fluxes of the riverine system. Formayer H. selected the climate episodes and helped to interpret the significance of the results. David L. produced the climate episode data and the upstream boundary water temperature. Kalny G. organized the field campaigns and built the basic vegetation and morphology data set. Trimmel H. further processed the data for the use of Heat Source, adapted and validated the model. She run the Heat Source simulations for all selected episodes and prepared the manuscript.

Acknowledgements: This research was part of the project BIO_CLIC and LOWFLOW+ both funded within the Austrian Climate Research Programme (ACRP) by the Klima und Energiefond. The regional climate model data sets used to produce the climate episodes were developed in the ENSEMBLES project supported by the European Commission's 6th Framework Programme through contract GOCE-CT-2003-505539. The INCA data set was created by the Zentralanstalt für Meteorologie und Geodynamik (ZAMG). Hydrological data and the digital elevation model were provided by hydrographic services, which are part of the Federal Ministry of Agriculture, Forestry, Environment and Water management and the federal state governmental geoinformation service authorities of Styria and Burgenland. Special thanks are given to the Oregon Department of Environmental Quality, who maintain the model Heat Source and opened the source code for scientific use.

References

Ahrens, B., Formayer, H., Gobiet, A., Heinrich, M., Hofstätter, M., Matulla, C., Prein, A.F. and Truhetz, H., et al. 2014. Kapitel 4: Zukünftige Klimaentwicklung, in: Österreichischer Sachstandsbericht Klimawandel, Wien, 301–346 pp., 2014.

APCC: Österreichischer Sachstandsbericht Klimawandel 2014 (AAR14), Helga Kromp-Kolb, Nebojsa Nakicenovic, Karl Steininger, Andreas Gobiet, Herbert Formayer, Angela Köppl, Franz Prettenthaler, Johann Stötter, and Jürgen Schneider (Hg.), Verlag der Österreichischen Akademie der Wissenschaften, Wien, Österreich, 1096 pp, 2014.

Arismendi, I., Safeeq, M., Dunham, J. B. and Johnson, S. L.: Can air temperature be used to project influences of climate change on stream temperature? Environ. Res. Lett., 9, 084015, doi:10.1088/1748-9326/9/8/084015, 2014.

Auer, I., Foelsche, U., Böhm, R., Chimani, B., Haimberger, L., Kerschner, H., Koinig, K. A., Nicolussi, K., Diendorfer, G. and Godina, R., et al. 2014. Kapitel 3: Vergangene Klimaänderung in Österreich, in: Österreichischer Sachstandsbericht Klimawandel 2014, p. 227–300.

Auer, I., Böhm, R., Jurkovic, A., Lipa, W., Orlik, A., Potzmann, R., Schöner, W., Ungersböck, M., Matulla, C., Briffa, K., Jones, P., Efthymiadis, D., Brunetti, M., Nanni, T., Maugeri, M., Mercalli, L., Mestre, O., Moisselin, J.-M., Begert, M., Müller-Westermeier, G., Kveton, V., Bochnicek, O., Stastny, P., Lapin, M., Szalai, S., Szentimrey, T., Cegnar, T., Dolinar, M., Gajic-Capka, M., Zaninovic, K., Majstorovic, Z. and Nieplova, E.,. HISTALP—historical instrumental climatological surface time series of the Greater Alpine Region. International Journal of Climatology 27, 17–46. doi:10.1002/joc.1377, 2007.

Beniston, M., Stephenson, D.B., Christensen, O.B., Ferro, C.A.T., Frei, C., Goyette, S., Halsnaes, K., Holt, T., Jylhä, K., Koffi, B., Palutikof, J., Schöll, R., Semmler, T., Woth, K., 2007. Future extreme events in European climate: an exploration of regional climate model projections. Climatic Change 81, 71-95. doi:10.1007/s10584-006-9226-z

Benyahya, L., Caissie, D., Satish, M.G. and El-Jabi, N.: Long-wave radiation and heat flux estimates within a small tributary in Catamaran Brook (New Brunswick, Canada), Hydrol. Process., 26, 475–484, 2012.

BMLFUW Abteilung I/4 – Wasserhaushalt, Hydrographisches Jahrbuch von Österreich 2013, Wien, 2015.

BMLFUW (Bundesministerium für Land- und Forstwirtschaft, Umwelt und Wasserwirtschaft, Eds.), Schöner, W., Böhm, R., Haslinger, K., Blöschl, G., Kroiß, H., Merz, R., Blaschke, A. P., Viglione, A., Parajka, J., Salinas, J. L., Drabek, U., Laaha, G. and Kreuzinger, N.: Anpassungsstrategien an den Klimawandel für Österreichs Wasserwirtschaft, Studie der Zentralanstalt für Meteorologie und Geodynamik und der Technischen Universität Wien, , Wien, 486 pp., 2011.

Boyd, M. and Kasper, B.: Analytical methods for dynamic open channel heat and mass transfer: Methodology for heat source model Version 7.0, available at: http://www.deq.state.or.us/wg/TMDLs/tools.htm, 2003.

Böhm, R.: ALP-IMP (EVK-CT-2002-00148) Multi-centennial climate variability in the Alps based on Instrumental data, Model simulations and Proxy data, final report for RTD-project, ZAMG, Central Institute for Meteorology and Geodynamics, Vienna, Austria, 2006.

Böhm, R.: Changes of regional climate variability in central Europe during the past 250 years, The European Physical Journal Plus, 127, doi:10.1140/epjp/i2012-12054-6, 2012.

Böhm, R., Auer, I., Schöner, W., Ganekind, M., Gruber, C., Jurkovic, A., Orlik, A. and Ungersböck, M.: Eine neue Webseite mit instrumentellen Qualitäts-Klimadaten für den Grossraum Alpen zurück bis 1760, Wiener Mitteilungen Band 216: Hochwässer: Bemessung, Risikoanalyse und Vorhersage, 2009.

Burn, D.H., and Hag Elnur, M.A, Detection of hydrologic trends and variability, J. Hydrol., 255, p107-122, 2002.

Caissie, D.: The thermal regime of rivers: a review, Freshw. Biol., 51, 1389–1406, doi:10.1111/j.1365-2427.2006.01597.x, 2006.

Caissie, D., Nassir, E.-J and Mysore, G. S.: Modelling of maximum daily water temperatures in a small stream using air temperatures, J. Hydology, 251, 14–28, 2001.

Caissie, D., Satish, M.G. and El-Jabi, N.: Predicting water temperatures using a deterministic model: Application on Miramichi River catchments (New Brunswick, Canada), J. Hydrol., 336, 303–315, 2007.

Chen, J., Franklin, J.F., Spies, T.A., Contrasting microclimates among clearcut, edge, and interior of old-growth Douglas-fir forest. Agricultural and Forest Meteorology 63, 219-237, 1993.

Capon, S. J., Chambers, L.E., Mac Nally, R., Naiman, R.J., Davies, P., Marshall, N., Pittock, J., Reid, M., Capon, T., Douglas, M., Catford, J., Baldwin, D.S., Stewardson, M., Roberts, J., Parsons, M. and Williams, S.E.: Riparian Ecosystems in the 21st Century: Hotspots for Climate Change Adaptation?, Ecosystems, 16, 359–381, doi:10.1007/s10021-013-9656-1., 2013

Clark, E., Webb, B.W. and Ladle, M.: Microthermal gradients and ecological implications in Dorset rivers, Hydrol. Process., 13, 423–438, 1999.

Cluis, D.: Relationship between stream water temperature and ambient air temperature – A simple autoregressive model for mean daily stream water temperature fluctuations, Nordic Hydrology 3 (2), 6571, 1972.

Cole, E. and Newton, M.: Influence of streamside buffers on stream temperature response following clear-cut harvesting in western Oregon, Canadian Journal of Forest Research 993–1005, 2013.

Davies-Colley, R. J. and Quinn, J. M.: Stream lighting in five regions of North Island, New Zealand: Control by channel size and riparian vegetation, N. Z. J. Mar. Freshw. Res., 32, 591–605, doi:10.1080/00288330.1998.9516847, 1998.

Déqué, M.: Frequency of precipitation and temperature extremes over france in an anthropogenic scenario: model results and statistical correction according to observed values, Glob Planet Change 57(1–2),16–26, 2007.

Dokulil, M.T.: Impact of climate warming on European inland waters, Inland Waters, 27–40, doi: 10.5268/IW-4.1.705, 2013

Ellenberg, H. and Leuschner, H: Vegetation Mitteleuropas mit den Alpen, 6.Auflage, Verlag Eugen Ulmer, Stuttgart, XXIV+1134pp, 2012.

Erickson, T. R. and Stefan, H.G: Linear Air/Water Temperature Correlations For Streams During Open Water Periods, Journal of Hydrologic Engineering, July 2000, 317 – 321, St. Anthony Falls Laboratory Technical Paper No. 604, Series A, 2000.

Garner, C.: Modeling the Effect of Riparian Shading on Water Temperature for Portions of the Carson River, Thesis, University of Nevada, Reno, USA, 2007.

Garner, G., Malcolm, I.A., Sadler, J.P. and Hannah, D.M.: What causes cooling water temperature gradients in a forested stream reach? Hydrol. Earth Syst. Sc., 11, 6441-6472, 2014.

Gobiet, A., Kotlarski, S., Beniston, M., Heinrich, G., Rajczak, J. and Stoffel, M.: 21st century climate change in the European Alps—A review, Science of The Total Environment, doi:10.1016 / j.scitotenv.2013.07.050, 2014.

Goler, R.A. and Formayer, H.: Temporal disaggregation of daily meteorological data to 15-minute intervals for use in hydrological models, in: EMS Annual Meeting Abstracts, Vol. 9, EMS2012-174-1. available at: http://meetingorganizer.copernicus.org/EMS2012/EMS2012-174-1.pdf, 2012.

Groom, J. D., Dent, L., Madsen, L.J. and Fleuret, J.: Response of western Oregon (USA) stream temperatures to contemporary forest management, For. Ecol. Manag., 262, 1618–1629, doi:10.1016/j.foreco.2011.07.012, 2011.

Guldenschuh, M.: Longitudial zonation of habitat parameters and fish species assemblages in the Austrian lowland rivers Lafnitz and Pinka, M.S. thesis, University of Natural Resources and Life Sciences, Vienna, 2015.

Haiden, T., Kann, A., Wittmann, C., Pistotnik, G., Bica, B. and Gruber, C.: The Integrated Nowcasting through Comprehensive Analysis (INCA) System and Its Validation over the Eastern Alpine Region, Weather Forecast., 26, 166–183, doi:10.1175/2010WAF2222451.1, 2011.

Hannah, D.M., Malcolm, I.A., Soulsby, C. and Youngson, A.F.: A comparison of forest and moorland stream microclimate, heat exchanges and thermal dynamics, Hydrol. Process., 22, 919–940, 2008.

Haylock, M.R., Hofstra, N., Klein Tank, A.M.G., Klok, E.J., Jones, P.D. and New, M.: A European daily high-resolution gridded data set of surface temperature and precipitation for 1950-2006, Journal of Geophysical Research, 113, D20119, doi:10.1029/2008JD010201, 2008.

Heino, J., Virkkala, R., and Toivonen, H., 2009: Climate change and freshwater biodiversity: detected patterns, future trends and adaptations in northern regions. Biol. Rev., 84, 39–54, doi:10.1111/j.1469-185X.2008.00060.x.

Holzapfel, G., Weihs, P., Rauch, H.P.: Use of the Shade-a-lator 6.2 model to assess the shading potential of riparian purple willow (Salix purpurea) coppices on small to medium sized rivers, Ecological Engineering, doi: 10.1016/j.ecoleng.2013.07.036, 2013.

Holzapfel, G. and Rauch H.P.: Der Einfluss der Ufervegetation auf die Wassertemperatur der Lafnitz und Pinka, Mitteilungsblatt für die Mitglieder des Vereins für Ingenieurbiologie, Ingenieurbiologie: Neue Entwicklungen an Fließgewässern, Hängen und Böschungen, 1/2015, 4–10, 2015.

Holzapfel, G., Rauch, H.P., Weihs, P. and Trimmel H.: The interrelationship of riparian vegetation and water temperature demonstrated with field data measurements and analysis of the rivers Pinka and Lafnitz, in: Geophysical Research Abstracts, 17, EGU General Assembly, Vienna, 12–17 April 2015, 11653–11653, 2015.

IPCC: The Physical Science Basis. Contribution of Working Group I to the Fifth Assessment Report of the Intergovernmental Panel on Climate Change, in: Climate Change 2013, T.F. Stocker et al. (Eds.), Cambridge University Press, Cambridge, United Kingdom and New York, NY, USA, 1535, 2013.

Johnson, S.L.: Factors influencing stream temperatures in small streams substrate effects and a shading experiment, Can.J.Fish.Aquat.Sci., 62, 913–923, 2004.

Johnson, M.F. and Wilby, R.L.: Seeing the landscape for the trees: metrics to guide riparian shade management in river catchments, Water Resour. Res., 51, 5, 3754-3769, doi:10.1002/2014WR016802, 2015.

Kalny, G., Dossi, F., Formayer, H., Graf, W., Leidinger, D., Leitner, P., Melcher, A., F. Pletterbauer, M. Seebacher, H. Trimmel, P. Weihs, H.P. Rauch: Das Potential der Ufervegetation zur Minderung von Effekten des Klimawandels auf biologische Lebensgemeinschaften kleiner bis mittelgroßer Fließgewässer, publizierbarer Endbericht BIO_CLIC ACRP, 42, Universität für Bodenkultur, Wien, 2015.

Kothandaraman, V.: Analysis of Water Temperature Variations in Large Rivers, ASCE Journal of Sanitary Engineering Division 97 (SA1), 1931, 1971.

Koutsoyiannis, D.: Rainfall disaggregation methods: Theory and applications, in: Proceedings of the Workshop on Statistical and Mathematical Methods for Hydrological Analysis, Universita degli Studi di Roma La Sapienza, Rome, 1-23, 2003.

Kurylyk, B. L., MacQuarrie, K. T. B., Caissie, D. and McKenzie, J. M.: Shallow groundwater thermal sensitivity to climate change and land cover disturbances: derivation of analytical expressions and implications for stream temperature modeling. Hydrol. Earth Syst. Sci., 19, 2469–2489, doi:10.5194/hess-19-2469-2015, 2015.

Kyselỳ, J., Kalvová, J. and Květoň, V: Heat waves in the south Moravian region during the period 1961-1995, Studia Geophysica et Geodaetica, 44, 57–72, 2000.

Leach, J.A. and Moore, R.D, Above-stream microclimate and stream surface energy exchanges in a wildfire-disturbed riparian zone. Hydrol Process. 24, 2369–2381, doi: 10.1002/hyp.7639, 2010.

Li G, Jackson CR, Kraseski KA (2012) Modeled riparian stream shading: Agreement with field measurements and sensitivity to riparian conditions. J Hydrol 428–429:142–151. doi: 10.1016/j.jhydrol.2012.01.032

Mader, H., Steidl, T., Wimmer, R., Ablussregime österreichischer Fliessgewässer. Umweltbundesamt/Federal Environment Agency - Austria, Wien, 1996.

Magnuson, J. J., Crowder, L. B. and Medvick, P.A.: Temperature as an Ecological Resource. Am. Zool. AmerZool, 19, 331–343, 1979.

Maheu A, Caissie D, St-Hilaire A, El-Jabi N (2014) River evaporation and corresponding heat fluxes in forested catchments, Hydrol Process 28:5725–5738. doi: 10.1002/hyp.10071

Matulla, C., Schöner, W., Alexandersson, H., Storch, H., Wang, X.L., 2008. European storminess: late nineteenth century to present. Clim. Dyn., 133-144. doi:10.1007/s00382-007-033

Matulla, C., Schmutz A., Melcher, A., Gerersdorfer, T. and Haas, P.: Assessing the impact of a downscaled climate change simulation on the fish fauna in an Inner-Alpine River, Int. J. Biometeorol., 52, 127–137, 2007.

Melcher, A., Pletterbauer, F., Kremser, H., and Schmutz, S.: Temperaturansprüche und Auswirkungen des Klimawandels auf die Fischfauna in Flüssen und unterhalb von Seen. Österr. Wasser- Abfallwirtsch., 65, 408–417, doi:10.1007/s00506-013-0118-y, 2013.

Melcher, A., Dossi, F., Wolfram Graf, Guldenschuh, M., Holzapfel, G., Lautsch, E., Leitner, P., Schaufler, K., Seebacher, M., Trimmel, H., Weihs, P., Rauch, H.P.: Assessment of aquatic habitat availability and climate change effects in medium sized rivers. 10th ISE Trondheim, Norway., 2014.

Melcher, A., Kalny, G., Dossi, F., Formayer, H., Graf, W., Pletterbauer, F., Schaufler, K., Trimmel, H., Weihs, P., and Rauch, H.P.: Der Einfluss der Ufervegetation auf die Wassertemperatur unter gewässertypspezifischer Berücksichtigung von Fischen und benthischen Evertebraten am Beispiel von Lafnitz und Pinka, Österreichische Wasser- und Abfallwirtschaft, doi: 10.1007/s00506-016-0321-8, 2016.

Mohseni, O., Stefan H.G. and Erickson T.R.: A nonlinear regression model for weekly stream temperatures. Water Resour. Res., 34, 2685–2692, 1998.

Moore, R. D., Spittlehouse D.L. and Story, A.: Riparian microclimate and stream temperature response to forest harvesting: a review, Journal of American water resources association (JAWRA), 813 – 834, 2005.

Muhar, S., Poppe, M., Egger, G., Schmutz, S., Melcher, A., Flusslandschaften Österreichs: Ausweisung von Flusslandschaftstypen anhand des Naturraums, der Fischfauna und der Auenvegetation. Bundesministerium für Bildung, Wissenschaft und Kultur, Wien, 2004.

Nachtnebel, H. P., Dokulil, M., Kuhn, M., Loiskandl, W., Sailer, R. and Schöner, W.: Der Einfluss des Klimawandels auf die Hydrosphäre. Österreichischer Sachstandsbericht Klimawandel 2014 (AAR14), Austrian Panel on Climate Change (APCC), Verlag der Österreichischen Akademie der Wissenschaften, Wien, Österreich, 411–466, 2014.

Pahr, A.: Geologische Karte der Republik Österreich, Blatt 137 Oberwart, Geologische Bundesanstalt, Wien, 1984.

Parker, F.L. and Krenkel, P.A.: Thermal pollution: status of the art, Department of Environmental and Resource Engineering, Vanderbilt University, Nashville, TN, 1969.

Pletterbauer, F., Melcher, A.H., Ferreira T. and Schmutz S.: Impact of climate change on the structure of fish assemblages in European rivers. Hydrobiologia, 744, 235–254, doi:10.1007/s10750-014-2079-y, 2015.

Radu, R., Déqué, M. and Somot, S.: Spectral nudging in a spectral regional climate model. Tellus Ser Dyn Meterol Ocean., 60, 898–910, 2008.

Rutherford, J.C., Blackett, S., Blackett, C., Saito, L. and Davies-Colley, R. J.: Predicting the effects of shade on water temperature in small streams, N. Z. J. Mar. Freshw. Res., 31, 707-721, 1997.

Salas, J.D., Delleur, J.W., Yevjevich, V. and Lane, E.L.: Applied Modelling of Hydrological Time Series, Water Resources Publications, Colorado, p.484, 1980.

Schaufler, K.: Water temperature effects on fish in pre-alpine, medium-sized rivers.M.S. thesis, University of Natural Resources and Life Sciences, Vienna, 2015.

Settele, J., Scholes, R., Betts, R., Bunn, S.E., Leadley, P., Nepstad, D., Overpeck, J.T. and Taboada, M.A.: Global and Sectoral Aspects. Contribution of Working Group II to the Fifth Assessment Report of the Intergovernmental Panel of Climate Change, in: Terrestrial and inland water systems. Climate Change 2014: Impacts, Adaptation, and Vulnerability, C.B. Field et al. (Eds.), Cambridge University Press, Cambridge, United Kingdom and New York, NY, USA, 271–359, 2014.

Sinokrot, B.A. and Stefan, H.G: Stream Temperature Dynamics: Measurements and Modeling, Water Resour. Res., 29, 2299-2312, 1993.

Skøien, J., Merz, R., and Blöschl, G., Top-Kriging – geostatistics on stream networks, Hydrol. Earth Syst. Sci., 10, 277-287, 2006.

Sridhar, V., Sansone, A. L., LaMarche, J., Dubin, T. and Lettenmaier, D. P.: Prediction of stream temperatures in forested watersheds, Journal of the American Water Ressources Association, 2004.

Trimmel, H., Gangneux, C., Kalny, G. and Weihs P.: Application of the model 'Heat Source' to assess the influence of meteorological components on stream temperature and simulation accuracy under heat wave conditions, Meteorol. Z. 25/4, 389–406, doi:10.1127/metz/2016/0695, 2016.

van Vliet, M. T. H., Ludwig F., Zwolsman J.J.G., Weedon G.P. and Kaba, P.: Global river temperatures and sensitivity to atmospheric warming and changes in river flow, Water Resour. Res., 47, W02544, doi:10.1029/2010WR009198, 2011.

van Vliet, M. T. H., Wiberg, D., Leduc, S. and Riahi, K.: Power-generation system vulnerability and adaptation to changes in climate and water resources. Nat. Clim. Change, doi:10.1038/nclimate2903, 2016.

Webb, B. W. and Nobilis F., 1995: Long term water temperature trends in Austrian rivers. Hydrol. Sci. J., 40, 83–96, doi:10.1080/02626669509491392.

Webb, B.W. and Nobilis, F.: Long-term perspective on the nature of the air-water temperature relationship: a case study. Hydrol. Process., 11, 137–147, 1997.

Webb, B. W., Hannah, D. M., Moore, D. R., Brown, L. E. and Nobilis, F.: Advances in Stream and River Temperature Research, Hydrol. Process., 22, 902-918, 2008

Wenger, S. J., Som, N.A., Dauwalter, D.C., Isaak D.J., Neville, H.M., Luce, C. H., Dunham, J.B., Young M.K., Fausch, K.D. and Rieman, B.E.: Probabilistic accounting of uncertainty in forecasts of species distributions under climate change, Glob. Change Biol., 3343-3354, doi:10.1111/gcb.12294, 2013.

WRG – Wasserrechtsgesetz (water right law), BGBI. Nr. 215/1959, 1959.

Table 1: Mean 5 day air temperatures of future heat wave episodes used as selection criteria, shown with equivalent values from the observed period for comparison.

	1a	5a	20a	Max
1981-2010 (“OBS“)	23.1	25.0	27.2	27.4
2016-2045 (“2030“)	23.4	26.6	27.2	29.0
2036-2065 (“2050“)	24.2	27.2	28.4	28.8
2071-2100 (“2085“)	28.1	30.6	31.0	32.0

Table 2: Mean and daily maximum air temperature, air humidity, wind speed, global radiation at the reference station and water temperature at the upstream model boundary averaged for the selected 5 day heat episodes in 2013 and the 1a, 5a, 20a and Max events of the climate periods centered on 2030, 2050 and 2085. For 2013 (OBS) measured values of the reference station 2m above the river (M.) and interpolated measurement data from the INCA (I.) data set are shown.

	OBS		2030				2050				2085			
	M.	I.	1a	5a	20a	max	1a	5a	20a	max	1a	5a	20a	max
Air temp. (mean) [°C]	26.2	27.2	23.3	26.6	27.2	29.0	24.2	27.2	28.4	28.8	28.1	30.6	31.0	32.0
Air temp (mean daily max) [°C]	34.5	35.7	30.0	33.7	34.6	37.5	29.5	33.7	35.9	36.9	34.8	38.2	39.6	39.0
Air humidity [%]	62	55	73	57	55	53	54	56	56	60	58	51	48	52
Wind speed [m s-1]	0.6	1.4	0.7	0.9	0.9	1.0	1.3	1.1	1.1	0.8	1.3	1.2	0.8	0.9
Global rad. [MJ m^{-2} d^{-1}]	24.6	24.6	23.4	25.0	28.0	29.0	24.9	28.7	23.1	21.7	27.3	24.5	23.8	20.9
Boundary water temperature [°C]	16.3	16.3	14.1	15.9	16.0	16.8	15.6	16.2	17.0	17.5	17.5	19.4	20.4	20.3

Table 3: Daily minimum, mean and maximum 5 day mean water temperature of the 5 day episodes averaged over the river Pinka. during the 1a, 5a and 20a episodes for the climate periods centered on 2030, 2050 and 2085 and mean low flow discharge at DFM 39. For 2013 (OBS), the measured values of the reference station 2 m above the river (Meas.) and interpolated measurement data from the INCA data set are compared.

	(a) max.			(b) mean			(c) min.		
	V0	STQ	V100	V0	STQ	V100	V0	STQ	V100
OBS Meas.	26.6	24.7	22.4	23.8	22.4	20.7	20.2	19.5	18.5
OBS INCA	26.1	24.4	22.1	23.7	22.5	20.8	21.0	20.1	19.2
2030_1a	24.5	23.1	20.7	21.5	20.4	18.6	16.5	16.5	16.3
2030_5a	25.9	24.3	22.1	22.5	21.3	19.7	17.8	17.2	16.5
2030_20a	27.0	25.0	22.5	22.2	22.4	20.2	19.4	18.2	17.2
2030_Max	27.2	25.7	23.5	24.8	23.4	21.6	21.9	20.8	19.5
2050_1a	24.3	22.6	20.0	21.6	20.4	18.9	19.0	18.2	17.3
2050_5a	26.5	24.8	22.2	23.7	22.3	20.5	20.4	19.5	18.4
2050_20a	26.6	24.8	23.0	23.7	22.6	21.3	20.2	19.9	18.9
2050_Max	27.5	25.9	23.7	25.1	23.9	22.2	22.5	21.5	20.4
2085_1a	28.6	24.9	23.1	26.2	22.5	21.7	22.3	18.8	18.8
2085_5a	29.0	27.3	25.0	26.5	25.3	23.7	24.1	23.0	21.7
2085_20a	28.9	27.3	25.5	26.7	25.5	23.9	23.6	22.9	21.7
2085_Max	29.3	27.8	25.7	27.1	26.0	24.6	25.0	24.1	23.0

Table 4: Difference to the 20a event of the OBS period (2013) (with mean low flow discharge) of predicted maximum (a), mean (b) and minimum (c) water temperatures for the 1a, 5a, 20a and Max event at DFS 39 for the climate periods centered on 2030, 2050 and 2085 for vegetation scenario V0 (no vegetation), STQ (vegetation unchanged), V100 (maximum vegetation).

	(a) max.			(b) mean			(c) min.		
	V0	STQ	V100	V0	STQ	V100	V0	STQ	V100
OBS INCA	1.7	0	-2.3	1.2	0	-1.7	0.9	0	0.9
2030_1a	0.1	-1.3	-3.7	-1	-2.1	-3.9	-3.6	-3.6	-3.8
2030_5a	1.5	-0.1	-2.3	0	-1.2	-2.8	-2.3	-2.9	-3.6
2030_20a	2.6	0.6	-1.9	0.3	-0.1	-2.3	-0.7	-1.9	-2.9
2030_Max	2.8	1.3	-0.9	2.3	0.9	-0.9	1.8	0.7	-0.6
2050_1a	-0.1	-1.8	-4.4	-0.9	-2.1	-3.6	-1.1	-1.9	-2.8
2050_5a	2.1	0.4	-2.2	1.2	-0.2	-2	0.3	-0.6	-1.7
2050_20a	2.2	0.4	-1.4	1.2	0.1	-1.2	0.1	-0.2	-1.2
2050_Max	3.1	1.5	-0.7	2.6	1.4	-0.3	2.4	1.4	0.3
2085_1a	4.2	0.5	-1.3	3.7	0	-0.8	2.2	-1.3	-1.3
2085_5a	4.6	2.9	0.6	4	2.8	1.2	4	2.9	1.6
2085_20a	4.5	2.9	1.1	4.2	3	1.4	3.5	2.7	1.6
2085_Max	4.9	3.4	1.3	4.7	3.5	2.1	4.9	4	2.9

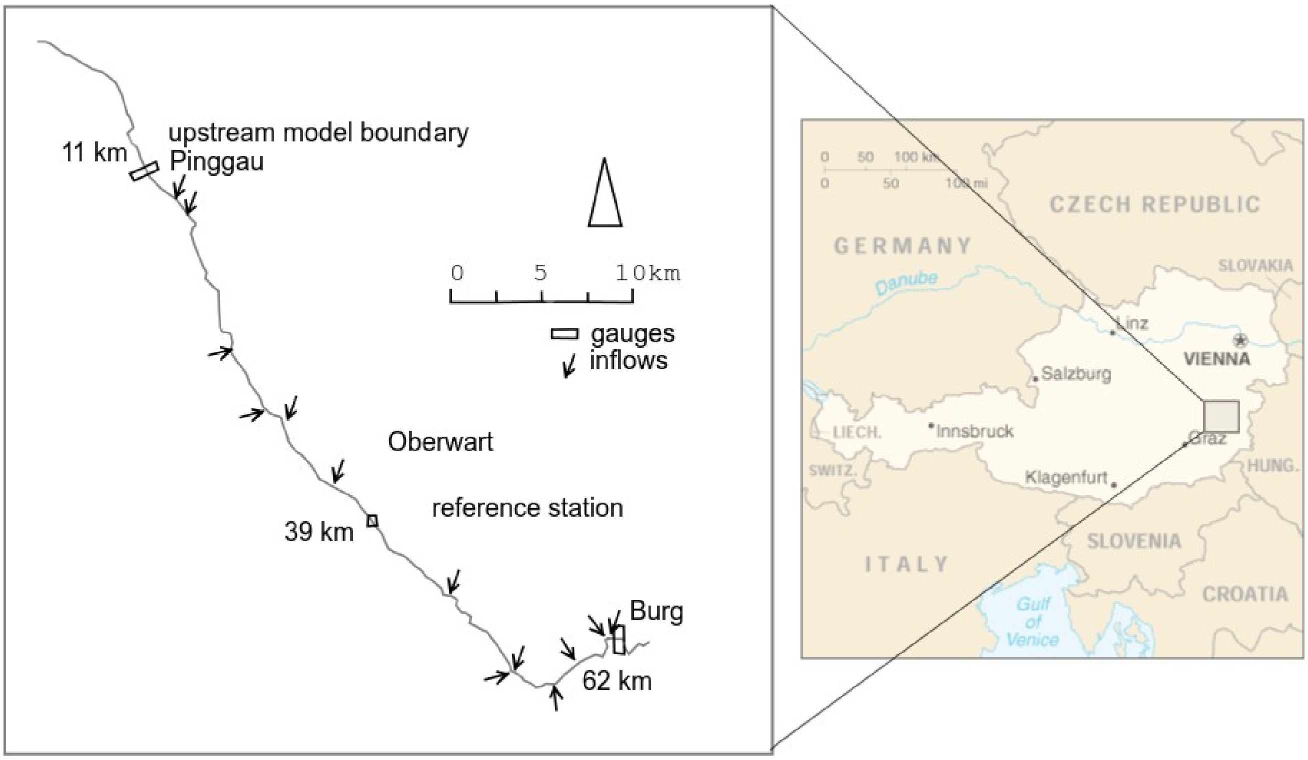

Figure 1: The study region in Pinka showing gauges, tributaries and the reference station (km markers shown as distance from source).

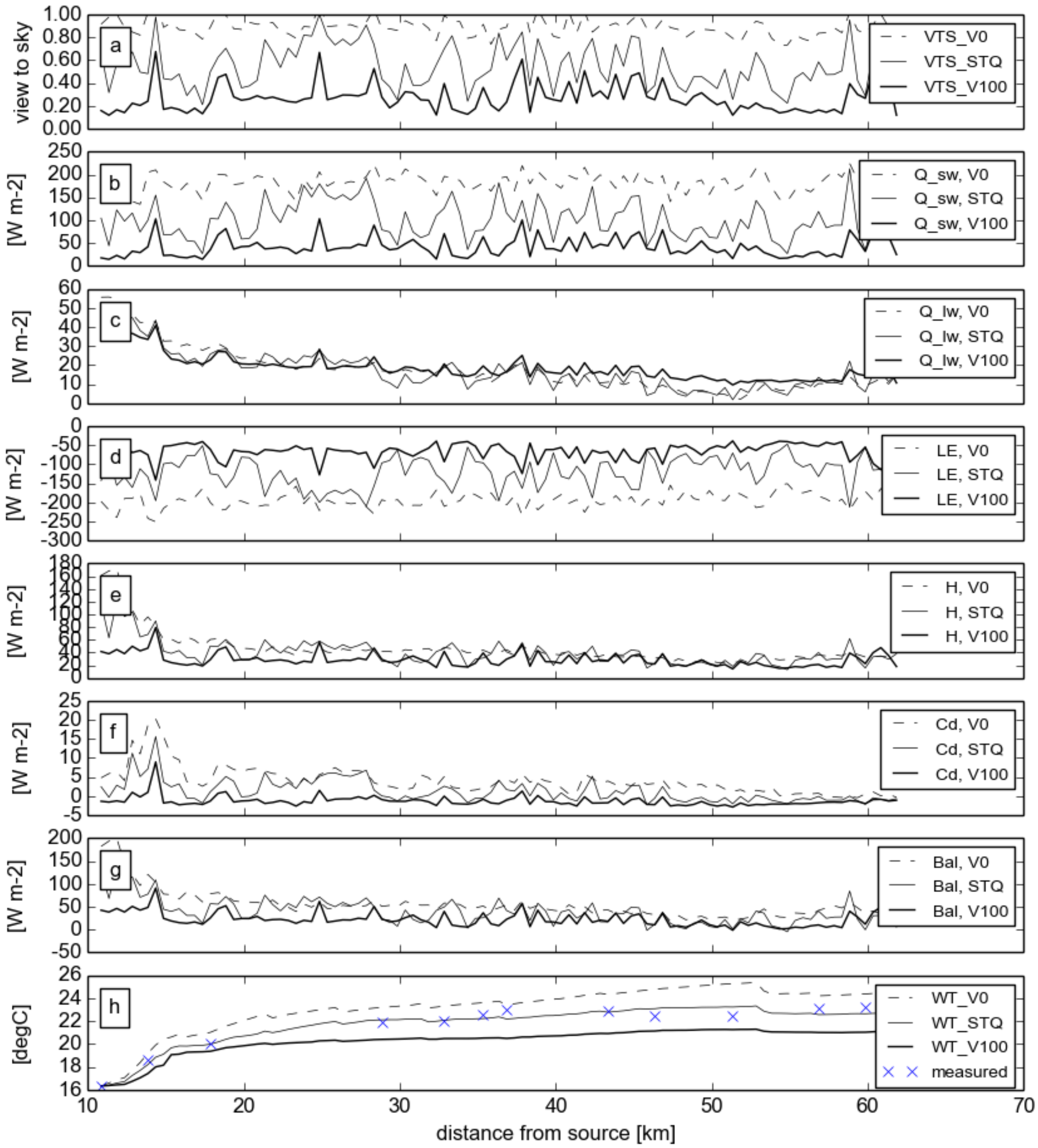

Figure 2: Comparison of the calculated VTS levels, short wave (Q_sw), long wave (Q_lw) radiation balance, latent (LE) and sensible (H) heat flux and measured (measured) and simulated (WT) water temperature for the heat wave episode 4 – 8 August 2013 along the river Pinka for three vegetation scnearios. no vegetation (V0), existing vegetation (STQ) and maximum vegetation (V100).

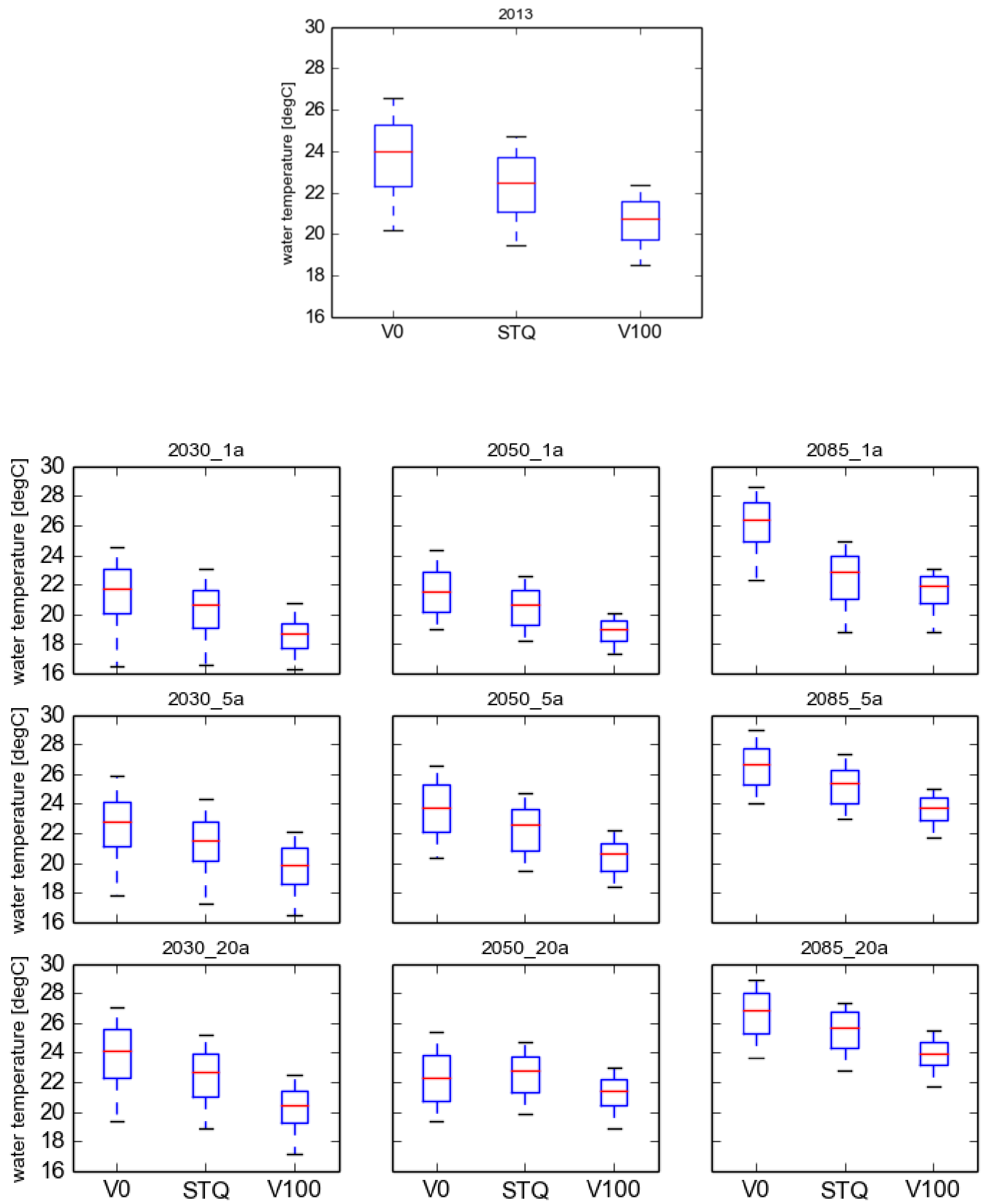

Figure 3: Box and whiskers chart showing the 5 day mean water temperature distribution during the 1a, 5a and 20a episodes for the climate periods centered on 2030, 2050, 2085 and mean low flow discharge at DFM 39.

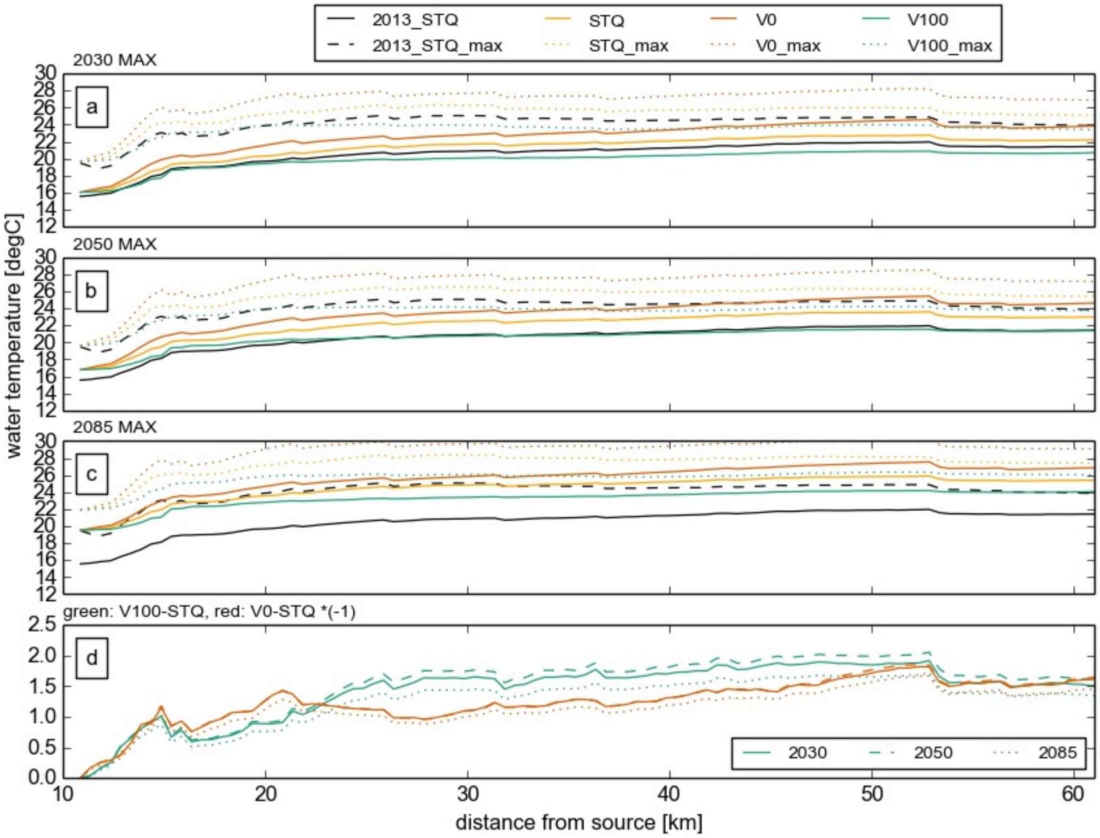

Figure 4: Mean and maximum water temperature averaged during the maximum events predicted for the climate periods centred on 2030, 2050 and 2085 along the river Pinka using vegetation scenarios V0, STQ and V100 in comparison to the maximum event recorded in 2013. The bottom panel shows the difference between STQ and V100 (green) and STQ and V0 (*-1) (red).